Available online www.jsaer.com

***Journal of Scientific and Engineering Research*, 2018, 5(7):283-292**

Research Article

ISSN: 2394-2630
CODEN(USA): JSERBR

Interpretation of the gravity anomaly map of the Sivas (Dumluca) - Turkey iron ore using the Cellular Neural Network (CNN) method

Ali Muhittin Albora

Istanbul University-Cerrahpaşa Department of Geophysics Engineering Avcilar, 34850, Istanbul, Turkey

Abstract A good distinction from potential anomaly maps and the identification of building boundaries is an important problem. In this way, the locations of the geological structures being sought can be determined precisely. In this article, the Cellular Neural Network (CNN) method is proposed in order to determine the structure boundaries and to distinguish between regional and residual anomalies. CNN provide fast and parallel computational capability for image processing applications due to its filtering structure. The behaviour of CNN is defined by two template matrices that are adjusted by a proper supervised learning algorithm. After training stage for geophysical data, Bouguer anomaly maps can be processed and analysed. CNN is employed to analyse Bouguer anomaly maps, which are important to extract useful information in geophysics. At first, CNN performance is tested on synthetic geophysical data, which are created by a computer. Then, Bouguer anomaly maps of Dumluca ore field has been analysed and results are reported comparing to real drilling results.

Keywords Bouguer anomaly maps, border detection, cellular neural network, Dumluca ore area

1. Introduction

The location of the boundaries of gravity and magnetic sources are important when investigating the geological setting of a region. Numerous techniques have been used for boundary analysis of gravity and magnetic anomalies. A well-known method of the horizontal location of source boundaries is to consider the zero contour of the second vertical derivative of gravity. Many methods have been devised for building boundaries based on different combinations of horizontal and vertical derivatives [1-4]. It has also been proven that the extensions of the maxima of the analytic signal amplitude correspond to the boundaries of the embedded structure [5-6]. In recent years, two and three dimensional studies can be done with wavelet method which is used as boundary detection and discrimination method [7-16]. They used the Steerable Filters technique, which is the current image processing method, in the determination of building boundaries [17-20]. They also used the Markov Random Filter technique to detect building boundaries [21-25]. Turkey's most important reserves of iron ore mined in the region where Bouguer anomaly map Research Institute of Mineral Research (MTA) was obtained by. The Cellular Neural Network (CNN) method has been applied in order to find possible mineral deposits in the Bouguer anomaly map. The map was then compared with the drilling data and the results were found to be successful.

Material and Method: *Cellular Neural Network (CNN)*

Cellular Neural Networks (CNN) is an analogue dynamic processor array which reflects the processing elements interact directly within a finite local neighborhood. It consists of simple processing elements (cells), usually placed in the nodes of an orthogonal or hexagonal grid, being connected to a set of nearest neighbors. In contrast the feed forward neural network, CNN employs two template matrices that are form of fix sized masks (Figure 1). The evaluation of a CNN is represented by a cell equation given either in the form of partial differential

equation of reaction-diffusion type, or in its finite-difference form, when all cells calculate their next states in parallel, iteratively and synchronously. The computation starts when all cells are set in an initial state, and it stops at a stable state, when no cells change their output states any more. Convergence to stable state of CNN depends on the suitable template coefficients and bias values inside the cells [25]. In addition to carrying some basic features of known artificial neural networks, they find a lot of applications in image processing and image recognition due to their two dimensional structure [26-30].

Definition : r-neighbourhood

The r-neighbourhood of a cell C*(i,j)* , in a cellular neural network is defined by,

$$N_r(i,j)=\left\{C(k,l)\middle|\max\{\,|k-i|,|l-j|\,\}\le r,1\le k\le M;1\le l\le N\right\}, \quad (1)$$

where *r* is a positive integer number.

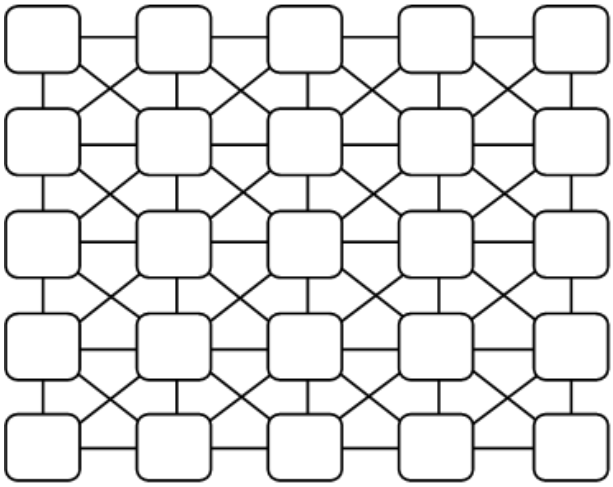

Figure 1: General CNN Neighbourhood Structure [27]

A general form of the cell dynamical equations may be stated as follows:

$$\frac{dx_{ij}(t)}{dt}=-x_{ij}(t)+\sum_{kl\in N_r(ij)}A_{(i-k)(j-l)}(t)\,y_{kl}+\sum_{kl\in N_r(ij)}B_{(i-k)(j-l)}(t)\,u_{kl}+I$$

$$y_{ij}(t)=f\left[x_{ij}(t)\right]=\frac{1}{2}\left(\left|x_{ij}(t)+1\right|-\left|x_{ij}(t)-1\right|\right) \quad (2)$$

For more information, see: [27-30],

with A, B and I being cloning template matrices that are identically repeated in the neighbourhood of every neuron as,

$$A=\begin{bmatrix}A_{-1,-1} & A_{-1,0} & A_{-1,1}\\ A_{0,-1} & A_{0,0} & A_{0,1}\\ A_{1,-1} & A_{1,0} & A_{1,1}\end{bmatrix},\quad B=\begin{bmatrix}B_{-1,-1} & B_{-1,0} & B_{-1,1}\\ B_{0,-1} & B_{0,0} & B_{0,1}\\ B_{1,-1} & B_{1,0} & B_{1,1}\end{bmatrix},\ \text{I}\ . \quad (3)$$

Synthetic Examples on CNN Approach

Thus the coefficients of A, B, and I templates are estimated and can be applied to separate residuel anomalies in real-time. Estimated CNN matrix elements of Equation (1) take the values as,

$$\text{A}=\begin{bmatrix}0 & 0 & 0\\ 0 & 0.03 & 0\\ 0 & 0 & 0\end{bmatrix}\qquad \text{B}=\begin{bmatrix}-1 & -1 & -1\\ -1 & 8 & -1\\ -1 & -1 & -1\end{bmatrix}\qquad \text{I= -1} \quad (4)$$

Table 1: Parameters of Bouguer anomaly map of Example 1

Parameters	Prisim 1	Prisim 2	Prisim 3	Prisim 4
(x) coordinates	(10.35)	(35.45)	(15.25)	(3.10)
(y) coordinates	(10.20)	(25.40)	(25.45)	(30.45)
h (uper depth)	5	3	4	2
H (Bottom depth)	10	8	9	5
δ (density)	1.5	1.8	1.6	1.5

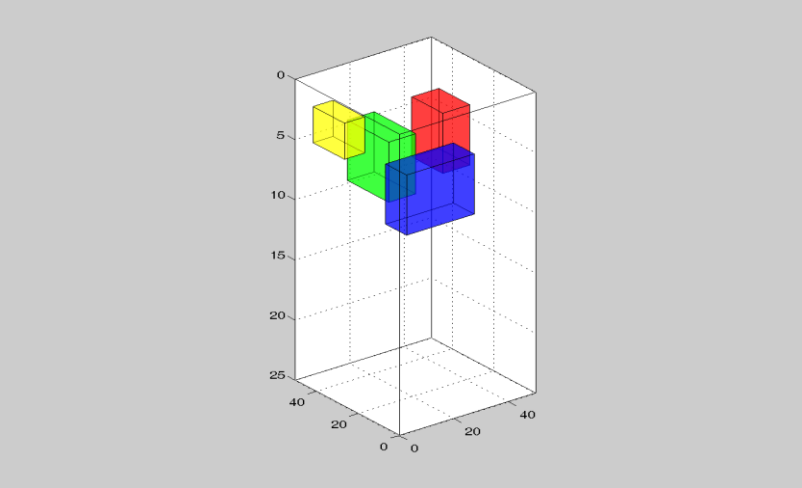

Figure 2: A synthetic model brought to you by four prisms

As a synthetic example (Table 1), the Bouguer anomaly map created by prisms with four different parameters is discussed (Figure 2). The purpose here is to determine the boundary of the structures of the prisms and to clarify the prisms closer to the surface. The Bouguer anomaly map, brought by four different prisms, is given in Figure 3a. The relief map of this map is shown in figure 3b. The horizontal gradient method is applied to these maps and the relief map is shown in Figure 3c. In addition, the hyperbola method is applied in figure 3d and relief map is given in 3e. Finally, a relief map of the CNN output is shown in FIG. 3g and a CNN output is shown at 3h.

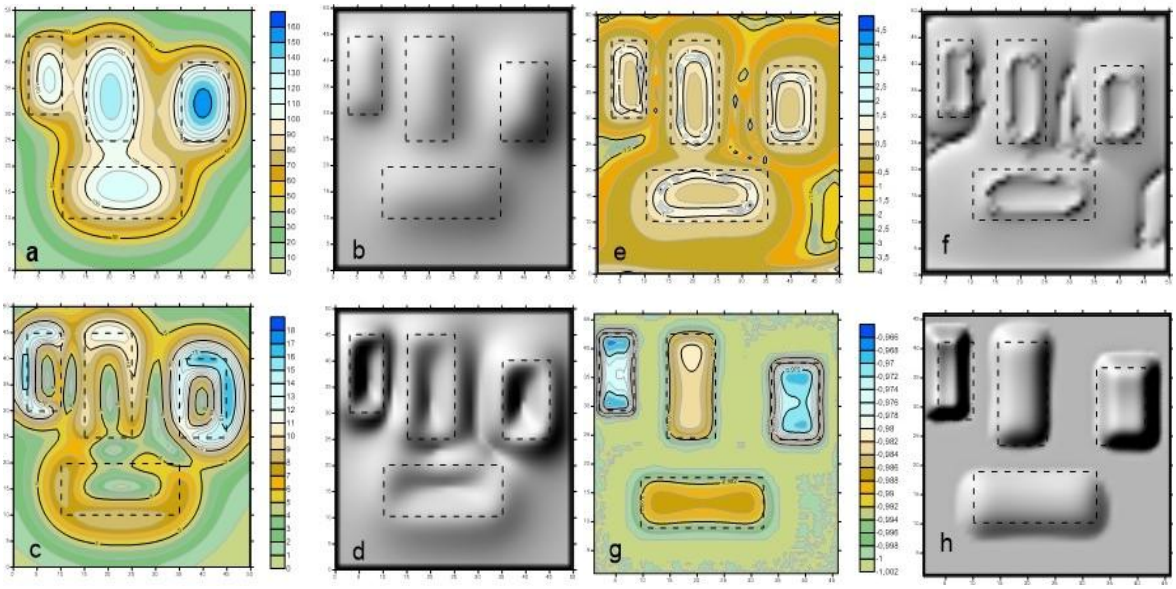

Figure 3: Synthetic a) Bouguer anomaly map (contour interval 10 mgal) b) Relief map. c) Horizontal gradient output of Bouguer anomaly map d) Horizontal gradient relief map e) Bouguer anomaly map hyperbolic output f) Hyperbolic relief map g) Bouguer anomaly map CNN output h) CNN output relief map

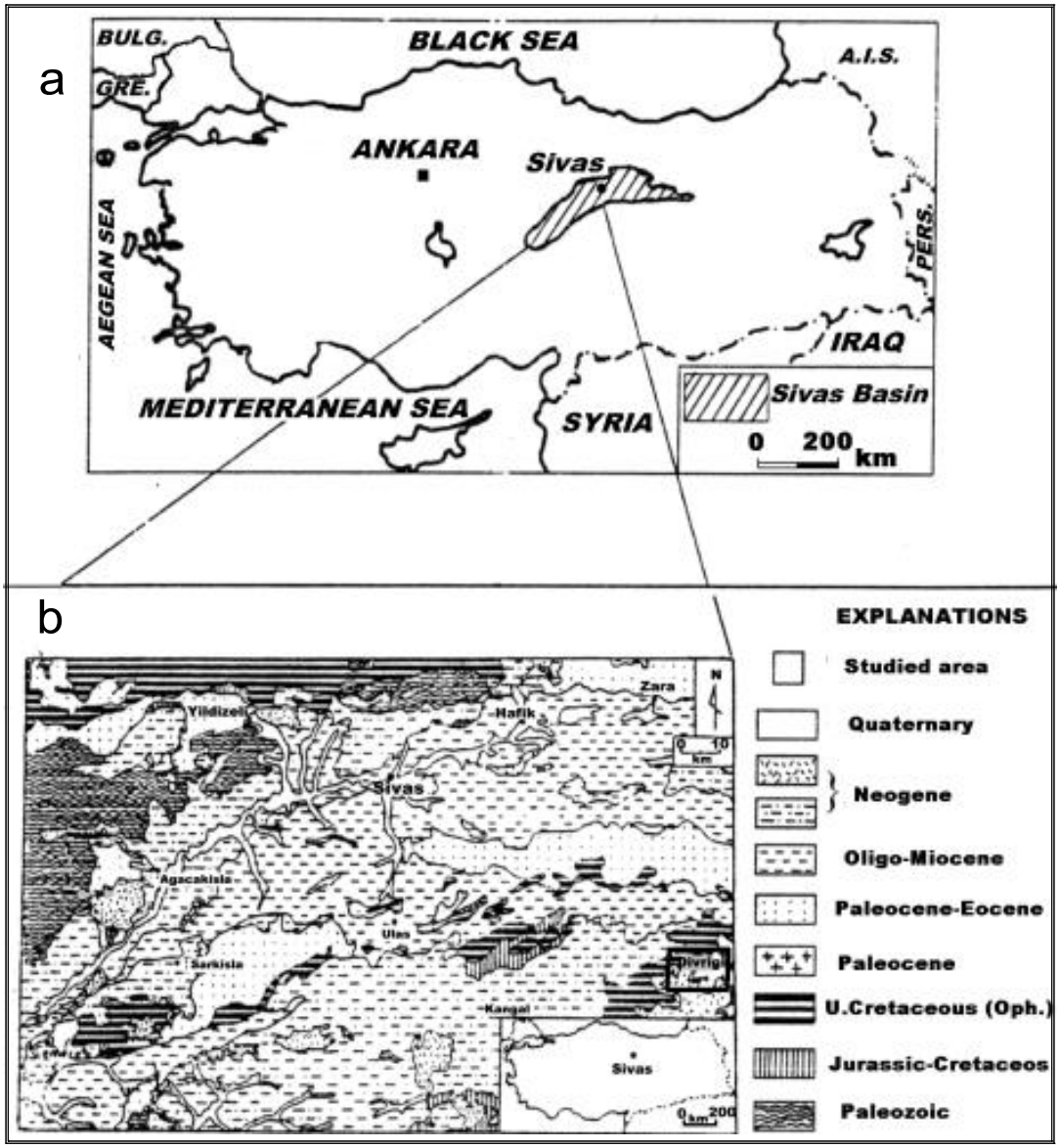

Figure 4: Working area a) Turkey-Sivas Dumluca iron ore b) Geology of the region [31]

Application of CNN method to Sivas-Dumluca iron ore area

Geology of the region:

Dumluca ore field is located in the northwest of Sivas, which is a city in Turkey (Figure 4a). The village of Dumluca is located in the north-western part of the province of Divriği in Sivas province. The region was located in the Tethys geosynclinals region along the Mesozoic. The marine limestone massifs formed in this period indicate this characteristic. The crystal of the geosynclinals base, which is not visible in the study area, should be Paleozoic. This Paleozoic basement has overturned to the north and south of the region. The orozygous development of the Mesozoic completed the Laramiende (Cretaceous end), and the Upper Cretaceous folds ascended to the terrestrial zone from deep-sea facies. The Paleocene kanglomals that come uncomfortably over the Cretaceous folds are in shallow sea character. In fact, these kanglomeralites cannot be distinguished precisely in the field of study, but are possible to see in the environment. Eocene Tethys is the result of re-flooding the sea, the region is a volatile geosyncline. In this era, it is seen that many regions that have risen so much in Laramie have stayed on the water in the islands. Nummulitic limestone's are formed in the deep parts of the sea and volcanic Eocene flysches are formed in the shallower parts. Eocene is mostly over older formations with a transgression. The Oligocene region is generally shallow marine, with variegated sandstones

and sometimes gypsiferous, saline floors. With the effect of radon orogeny developing after the Miocene, both the Miocene folds and the Miocene sea retreats.

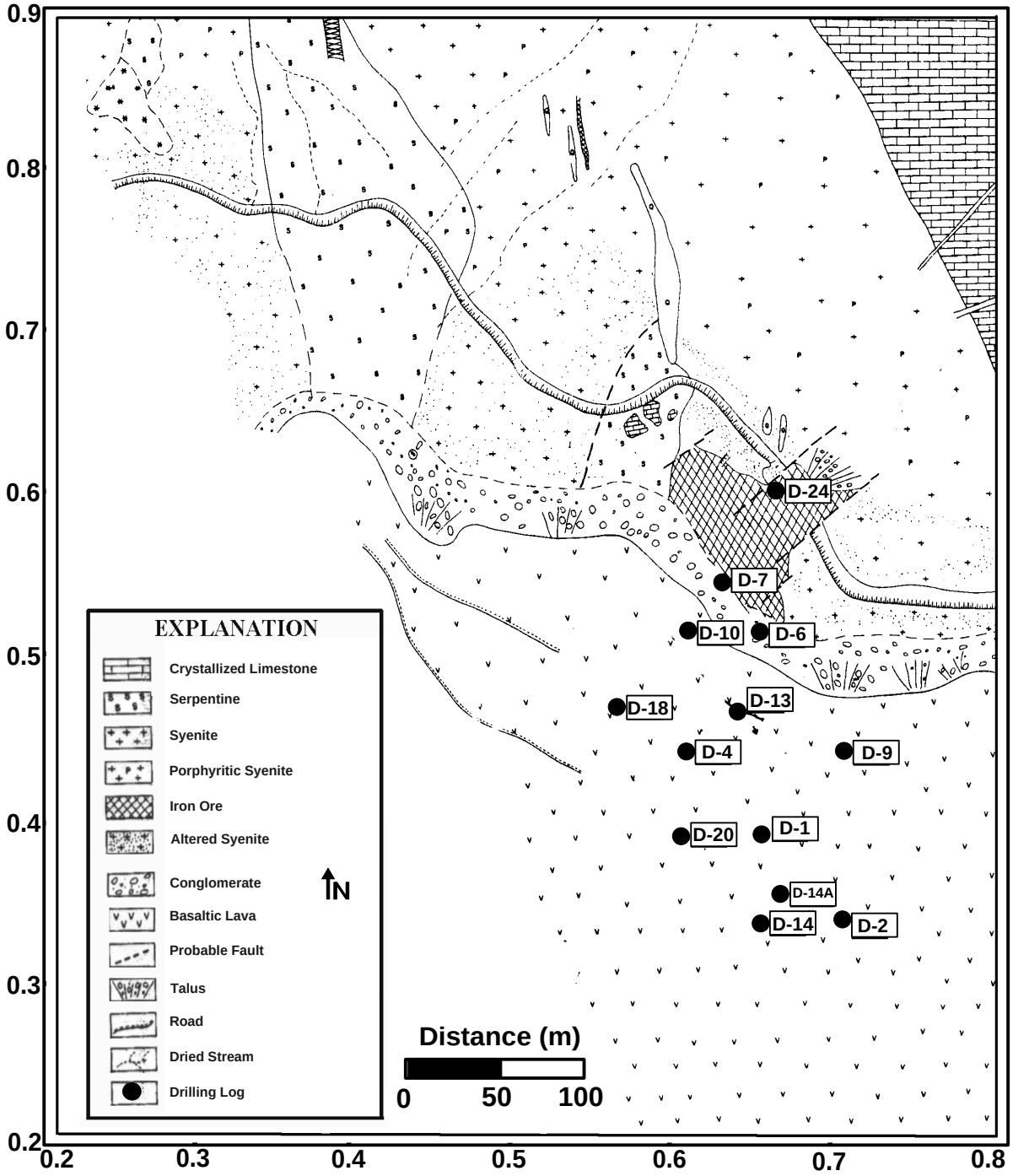

Figure 5: Geological map of Dumluca region (Modified by quotation) [33]

After that, in the territory turned into land, large and thick conglomerate floors were formed with a rainy climate effect. These conglomerates formed thick masses in the pits where the ancient Miocene marine was located [32]. The region is located on the east of the Taurus Mountains. A large part of the area contains blocks of various age types and sizes, units belonging to the Bozkir Unit consisting of rocks (allokton) units. These units contain ophiolite blocks, tuffs and basic submarine volcanics of varying sizes.The oldest rock unit in the region is composed of Permian aged, quartzite calcschist, phyllite and dolomitic limestone which are exposed in the vicinity of Bakır Tepe in the north of Alacahan. The Mesozoic in the region is a thick sediment consisting of

thick sedimentary carbonates. The granitic rocks did not bring up ore solutions, as they used to be, and they formed the hornfels zones by influencing the side rocks with some liquids and by moving the waters in the side rock by heat effect, they formed beds by moving the demagnetizations in serpentinized basic and ultrabasic rocks (Figure 4b). In Plio-Quaternary tuff, tuffite, anglomera and basalts spread especially around Dumluca [32].

The serpentinized basic and ultra-basic rocks form the source of iron ores in the region. Granitic rocks have not brought out ore solids as we once thought. The hornfels zones formed by influencing the side rocks with some liquids and the waters in the side rocks were serpentinized by the effect of heat again. The debris in the basic and ultrabasic rocks keeps the beds from moving. In Plio-Quaternary tuff, tuffite, anglomera and basalts spread around Dumluca (Figure 5) [33].

Soundings in Dumluca area

The first sounding work on the bed was made in 1969. Soundings of D-1, D-2 and D-4 were carried out by the MTA in 1970. In 1976, MTA and Turkey Iron and Steel işletmesitdc negotiated the drilling program have been implemented. During this period, drillings of D-10, D-13, D-14, D-14A, D-18, D-20 and D-24 were made. In these drillings, the ore was not cut in D-18 and D-9. It is not seen on the crystallized limestone surface, but it is cut into bands 5-10 meters in thickness between 36-112 meters in the sounding of D-7. At D-18 sounding, 3.25 meters massive pyrrhotite (less nickel and cobalt) was observed between 184 and 190 meters (Figure 6).

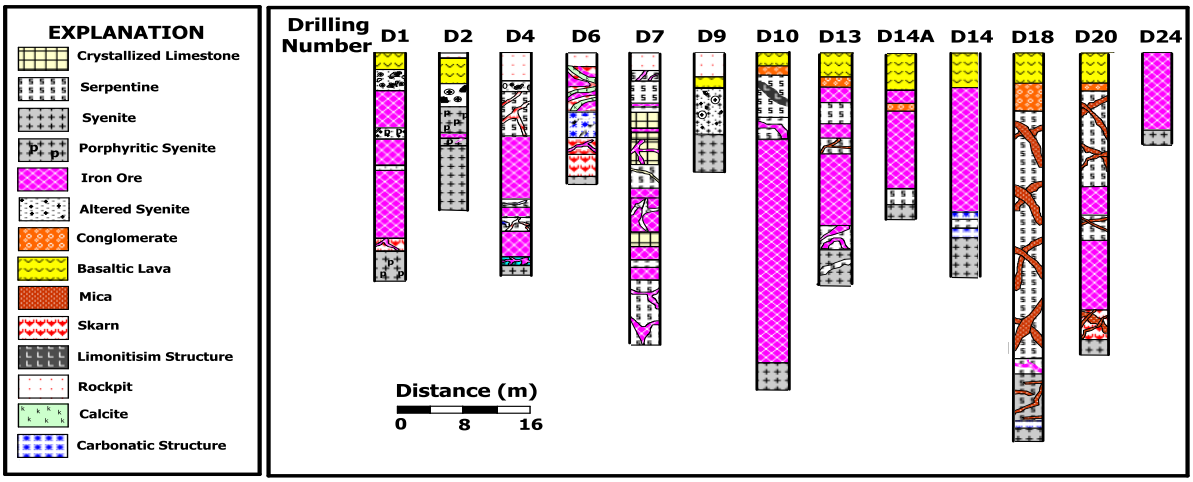

Figure 6: Drilling Logs of the Dumluca iron ore reserves [33]

The thickness of the cover of Pliocene conglomerate and basalts above the ore level in the Dumluca iron bed is low. The thickness of this covering covering a large part of the bed is 20-30 m. between. This covering layer is greater than the slope of the bed towards the west towards the D-18 sounding. This thickness is 80 m. In D-20 sounding, 54 m. In D-4, 40 m. In D-10. It is up. Ore = 0.55 was found. The ore is pyritic magnetite, martitized at upper levels. The average sulfur content is between 1.5% and 2%, and direct sarja is available. Copper, nickel, and cobalt are present in the trivial situation. Chemical analyzes show that other sulfur minerals other than pyrite will not degrade the ore quality [33].

Dumluca Mining bed formation

The Dumluca iron bed is a typical pyro metasomatic or skarn type bed, and it is found that it is limited by faults from three sides with tectonism after ore mineralization. It is thought that the boundaries of Dumluca iron ore are not natural and a large part of the bed can be detected is still not revealed [32].

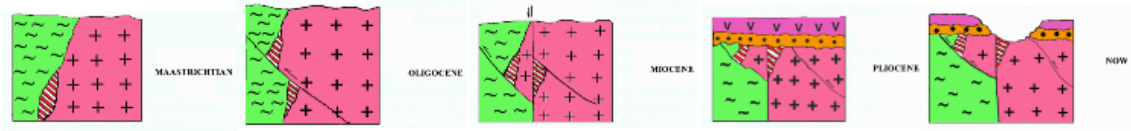

Figure 7: Estimated tectonic evolution of the Dumluca Mine bed [32]

This view can be seen in the upper Miocene Pliocene aged detritus in the case of overlay or pickling material of the ore. The conglomerates, which slope westward at an angle of about 5 degrees, contain large ore pebbles. These ore pebbles are thought to have been transported from the south. Today, the southern part is covered with basalt lavas in the upper Miocene ages. As a result, under the basalt lavas in the south and the south-east, the original position of the ore body may occur under the menonite and serpentine hot contact. Figure 7 shows the predicted tectonic evolution of the bed after its formation [32].

Geophysical studies in the region

A map of gravity anomaly was obtained by the Mineral Research and Exploration Institute (MTA) at Dumluca mine site (Figure 8). When looking at the Bouguer anomaly map, two different anomalous sites are visible. Anomaly values increase as the center approaches east. The Dumluca Bouguer anomaly map continues with an increase of 5.6 mgal toward the center, starting at 2.4 mgal. On the Bouguer anomaly map, drilling locations are also shown. The CNN method was applied to the Bouguer anomaly map (Figure 9).

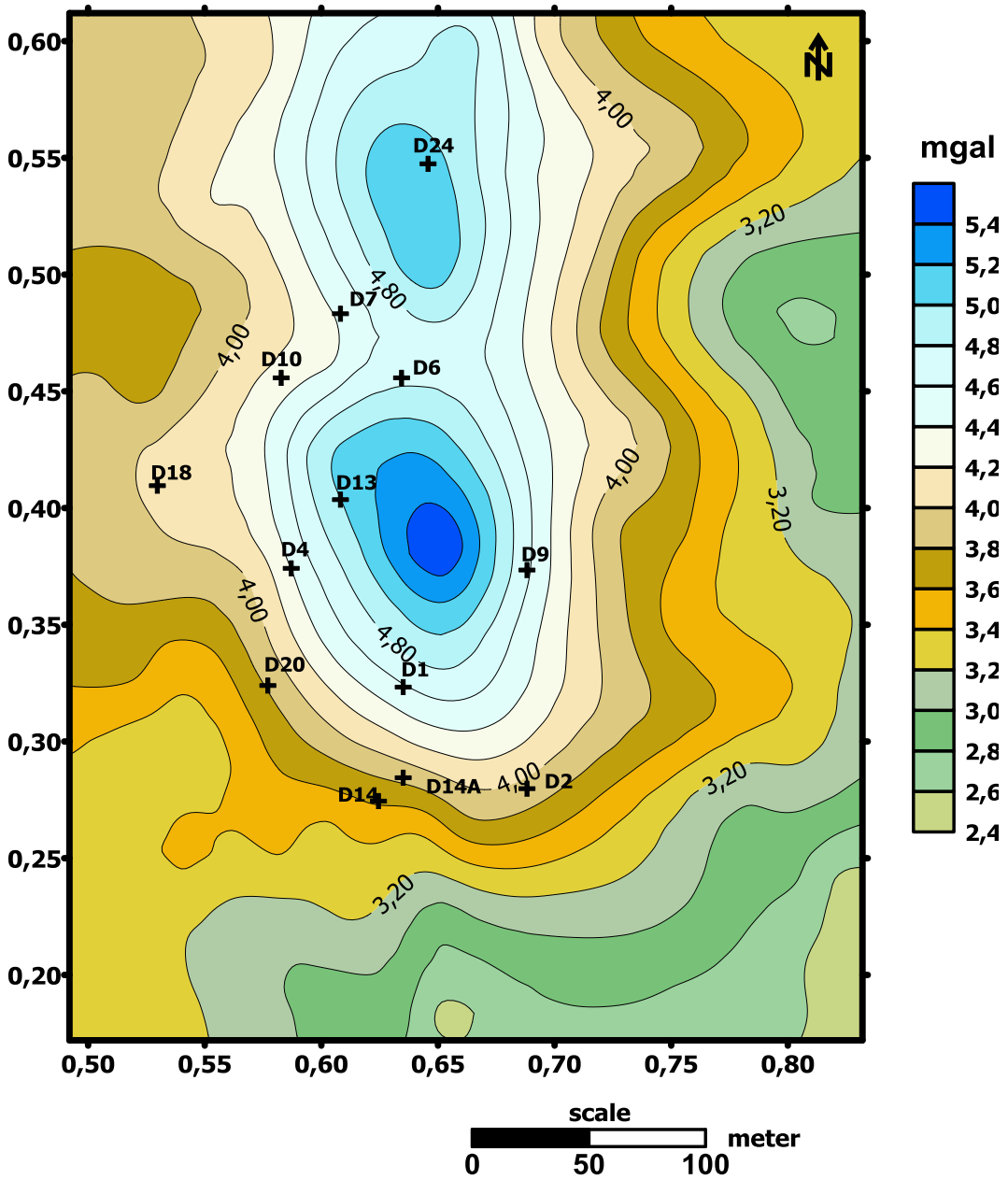

Figure 8: Gravity anomaly map of Dumluca iron ore area (contour interval is 0.2 mGal)

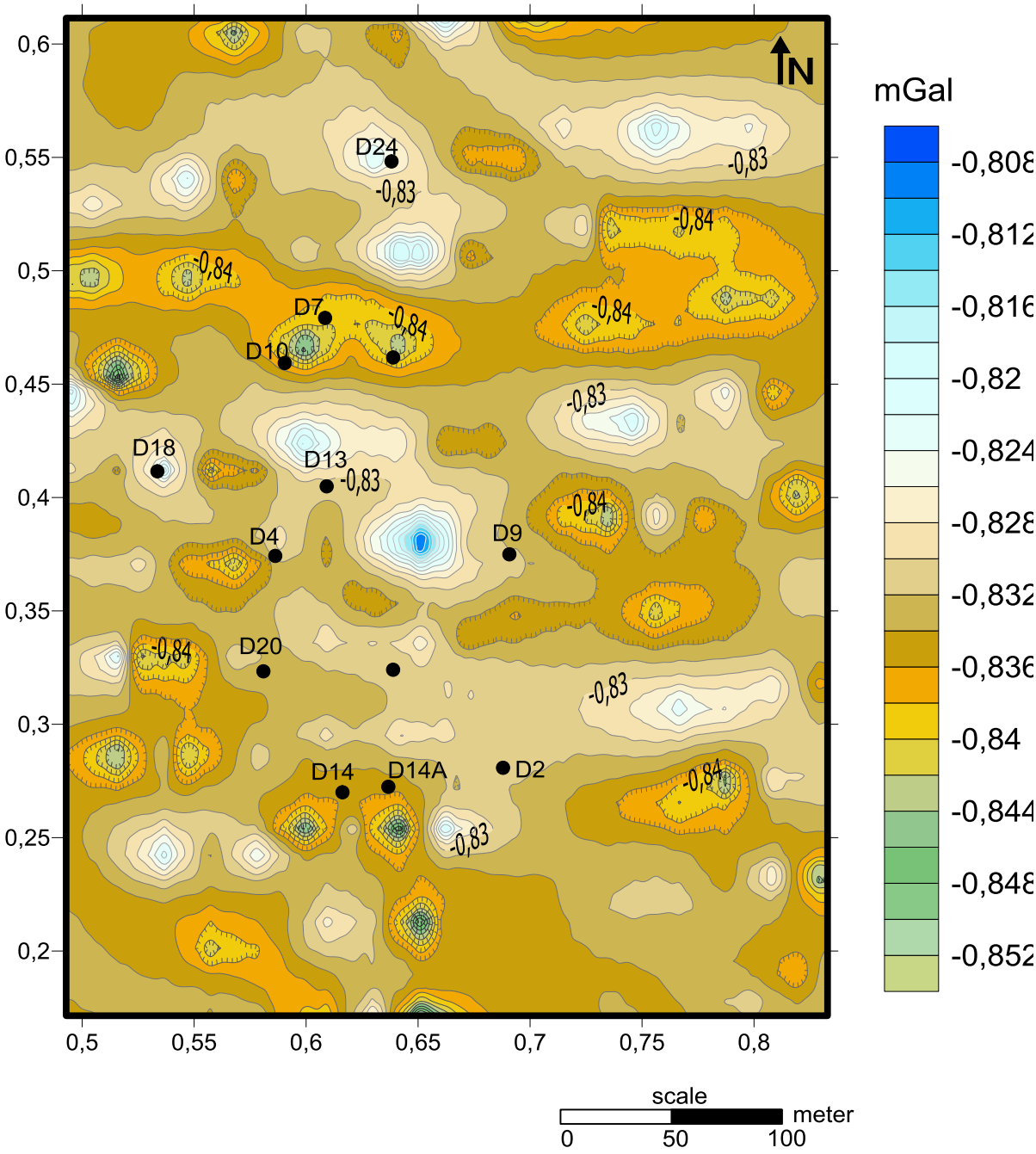

Figure 9: CNN output of Bouguer anomaly map of Dumluca Iron ore

Results and Discussion

When looking at the CNN output of the Bouguer anomaly map, no anomaly was observed in the D-2 and D-9 drilling areas, and no metal was found in the drillings (Figure 9). Although there is no anomaly at the CNN exit of the site where the D-18 borehole is located, it appears that the basaltic lava in this place is caused by the effect of canglomerate. The anomaly effect is also observed in the place where the D-24 bore is located, and this location is very close to the surface of the mine. D-14 and D14A are located just below the mine basalt lava in the drilling sites.The thickness of the cover of Pliocene conglomerate and basalts above the ore level in the Dumluca iron bed is low. The thickness of this veil covering most of the bed is 20-30 m. between. Only the D-18 sounding goes beyond the fact that the bed is plunging to the west. In D-20 sounding this thickness is 80 m. 54 m in D-4. 40 m in D-10.

Acknowledgement

This research was supported by Research Institute of Istanbul University (The Project Number: 1247/050599). The authors wish to thank MTA for providing of potential field data for this study.

References

[1]. Nabighian, M.N., (1984). Toward a three dimensional automatic interpretation of potential field data via generalized Hilbert Transforms: Fundamental relations. *Geophysics*, 49, 780-786.

[2]. Nelson, J.B., (1988). Calculation of the magnetic gradient gradient tensor from total field gradient measurements and its application to geophysical interpretation. *Geophysics*, 53, 957-966.

[3]. Roest, W.R., Verhoef, J. and Pilkington, M., (1992). Magnetic interpretation using the 3-D analytic signal. *Geophysics*, 55, 116-125.

[4]. Blakely, R.J., (1996). Potential theory in gravity and magnetic applications. Cambridge University Press, Cambridge, 441 pp.

[5]. Nabighian, M.N., (1972). The analytic signal of two-dimensional magnetic bodies with polygonal cross-section: Its properties and use for automated interpretation. *Geophysics*, 37, 507-517.

[6]. Akyol, N., (2016). Different Edge Detection Techniques for Imaging Buried Geological Structures. *Bulletin of the Earth Sciences Application and Research Centre of Hacettepe University.* 37 (3), 253-270.

[7]. Fedi, M. and Quata, T. (1998). Wavelet Analysis for the regional-residual and local seperstion at potential field anomalies. *Geophysical Prospecting*, 46, 507-525.

[8]. Uçan, O.N., Şeker, S., Albora, A. M. and Özmen, A. (2000). Separation of Magnetic Field Data Using 2-D Wavelet approach. *Journal of the Balkan Geophysical Society*, 3, 53-58.

[9]. Uçan, O.N. Albora, A.M. and Hisarlı, Z.M. (2001). Comments on the Gravity and Magnetic Anomalies of Saros Bay using Wavelet approach. *Marine Geophysical Researches*, 22, 251-264.

[10]. Daubechies, L. (1990). The Wavelet Transform, Time-Frequency Localization and Singnal Analysis. IEEE Trans. on Information Theory, 36.

[11]. Oruç, B. (2014). Structural interpretation of south part of western anatolian using analytic signal of the second order gravity gradients and discrete wavelet transform analysis. *Journal of Applied Geophsics*, 103, 82-98.

[12]. Albora, A.M and Uçan, O.N. (2001). Gravity Anomaly Separation Using 2-D Wavelet Approach and average depth calculate. *Dogus Magazine-Dogus University*, 3, 1-13.

[13]. Albora, A. M., Hisarlı, Z. M. and Uçan, O. N. (2004). Application of Wavelet Transform to Magnetic Data Due to Ruins of Hittite Civilization in Turkey. *Pure and Applied Geophysics*, 161, 907-930.

[14]. Alp, H. and Albora, A. M. (2009). Tracing of East Anatolian Fault Zone by using Wavelet analysis method. *e-Journal of New World Sciences Academy* Vol: 3, Issue: 2, Pages: 151-167.

[15]. Albora A.M. (2014). Wavelet Method Approach of Archaeogeophysics Studies., *Signal Processing and Communication Application Conference (SIU)*, 2016 22th, 514-517.

[16]. Albora A.M., (2018). Detection of building boundaries in mine fields using wavelet method. *Journal of Scientific and Engineering Research*, 5 (3), 407-414, 2018.

[17]. Özmen, A., Uçan, O. N. and Albora A. M. (2002). Boundary Detection Using Steerable Filters. *The 2nd International Conference on Earth Sciences and Electronics (ICESE-2002)*. V 2, 263-268.

[18]. Ucan, O. N., Albora, A. M. and Ozmen, A. (2003). Evaluation of Tectonic Structure of Gelibolu (Turkey) Usıng Steerable Fılters. *Journal of the Balkan Geophysıcal Socıety*, 6, 4, 221 – 234.

[19]. Albora, A. M., Say, N., Ucan, O. N. (2006). Evaluation of Tectonic Structure of İskenderun Basin (Turkey) Using Steerable Filters. *Marine Geophysical Researches*, 27, 225-239.

[20]. Görgün E., Albora A.M., (2017). Seismotectonic Investigation of Biga Peninsula in SW Marmara Region Using Steerable Filter Technique, Potential Field Data and Recent Seismicity. *Pure and Applied Geophysics*, 174, 3889-3904.

[21]. Uçan O.N. and Albora, A. M. (2001). Evaluation of Akdag Iron Ore Reserves Using Differential Markov Random Field (DMRF). *Journal of the Balkan Geophysical Society*, 4, 101-110.

[22]. Albora, A. M., Ucan, O. N. (2006). Separation of Magnetic Field Data Using Differential Markov Random Field (DMRF) Approach. *Geophysics*, 71, 125-134.
[23]. Albora, A. M., Ucan, O. N., Aydoğan, A. (2007). Modeling Potential Fields Sources In The Gelibolu Peninsula (Western Turkey) Using A Markov Random Field Approach, *Pure and Applied Geophysics*, 164, 1057-1080.
[24]. Uçan, O.N. and Albora, A. M. (2009). Evaluation of Ruins of Hitit Empire In Sivas-Kusakli Region using Markov Random Field (MRF), *Near Surface Geophysics*, 7, 2, 111-122.
[25]. Albora A.M., (2017). Investigation of Tectonic Structure of Turkey-Hatay Region Using Markov Random Fields (MRF), *Journal of Scientific and Engineering Research*, l.4, 86-93.
[26]. Chua L.O. and Yang L., (1988). Cellular Neural Networks: Theory, *IEEE Transactions on Circuits and Systems*, 35 (10), 1257 – 1272, 1988.
[27]. Albora, A. M., Uçan, O.N., Özmen A. and Özkan, T. (2001a). Separation of Bouguer anomaly map using cellular neural network. *Journal of Applied Geophysics*, 46, 129-142.
[28]. Albora, A. M. Özmen, A. and Uçan., O. N. (2001b). Residual Separation of Magnetic Fields Using a Cellular Neural Network Approach. *Pure and Applied Geophysics*, 158, 1797-1818.
[29]. Uçan, O.N., Bilgili, E. and Albora, A.M. (2002). Magnetic Anomaly Separation using Genetic Cellular Neural Networks. *Journal of the Balkan Geophysical Society*, 5, 65-7.
[30]. Bilgili, E. Göknar, Z. C. Albora, A. M. and Ucan O.N. (2005). Potential anomaly separation and archeological site localization using genetically trained Multi Level-Cellular Neural Network, *ETRI Journal*, 27, 3, 294-303.
[31]. Albora, A. M., Bal, A., Ucan, O. N. (2007). A new approach for border detection of Dumluca (Turkey) iron ore area: Wavelet Cellular Neural Networks. *Pure and Applied Geophysics*, 164, 119-215.
[32]. Öztürk, H. (1991). Divrigi ore province and source comments: Ph.D. Thesis, Istanbul University, Science and Technology Institute.
[33]. Yıldız, N. (1977). Drilling Report of Divrigi-Dumluca Iron Ore, MTA Report No. 315, Ankara.